Altered Order of Substrate Binding by DNA Polymerase X from African Swine Fever Virus†

Sandeep Kumar,‡ Marina Bakhtina,‡ and Ming-Daw Tsai*,‡,§

Department of Chemistry, The Ohio State University, Columbus, Ohio 43210, and Genomics Research Center and Institute of Biological Chemistry, Academia Sinica, Taipei 115, Taiwan

Received April 24, 2008; Revised Manuscript Received May 29, 2008

ABSTRACT: A sequential ordered substrate binding established previously for several DNA polymerases is generally extended to all DNA polymerases, and the characterization of novel polymerases is often based on the assumption that the enzymes should productively bind DNA substrate first, followed by template-directed dNTP binding. The comprehensive kinetic study of DNA polymerase X (Pol X) from African swine fever virus reported here is the first analysis of the substrate binding order performed for a low-fidelity DNA polymerase. A classical steady-state kinetic approach using substrate analogue inhibition assays demonstrates that Pol X does not follow the bi-bi ordered mechanism established for other DNA polymerases. Further, using isotope-trapping experiments and stopped-flow fluorescence assays, we show that Pol X can bind Mg^{2+}•dNTPs in a productive manner in the absence of DNA substrate. We also show that DNA binding to Pol X, although rapid, may not always be productive. Furthermore, we show that binding of Mg^{2+}•dNTP to Pol X facilitates subsequent formation of the catalytically competent Pol X•DNA•dNTP ternary complex, whereas DNA binding prior to dNTP binding brings the enzyme into a nonproductive conformation where subsequent nucleotide substrate binding is hindered. Together, our results suggest that Pol X prefers an ordered sequential mechanism with Mg^{2+}•dNTP as the first substrate.

DNA polymerases constitute an important class of enzymes and are required for genomic replication and maintenance. They catalyze template-directed nucleotidyl transfer reaction where a nucleotide (dNTP) is added to the 3′-OH terminus of a primer strand. Consistent with their importance to the viability of organisms, the function, structure, mechanism, and fidelity of DNA polymerases have been a focus of active research for several decades. In the early going, researchers established the order of DNA and dNTP substrate binding for several DNA polymerases. For example, steady-state kinetic studies showed that the substrate binding by Klenow fragment of *Escherichia coli* DNA polymerase I (Pol[1] I) is strictly ordered: the enzyme binds DNA first, followed by dNTP (*1*). Kinetic analyses of mammalian polymerases α and β and HIV reverse transcriptase also suggested the same sequential ordered mechanism in which DNA binding always occurs before productive dNTP binding (*2–5*). Structural studies have demonstrated that even though DNA polymerases can form binary complexes with dNTPs, the positioning of the substrate in the active site greatly differs from the catalytically potent conformation, which suggests nonproductive or adventitious substrate binding (*6, 7*). Furthermore, isotope-partitioning experiments using Pol I have demonstrated the catalytic incompetence of the E•dNTP binary complex, which in turn implies that any E•dNTP complex that may form must dissociate before DNA binding. It was also shown in the same studies that the enzyme should first form a productive binary complex with DNA substrate, followed by dNTP binding, for catalysis to occur (*8*).

On the basis of the aforementioned studies, it is generally assumed that all DNA polymerases possess the same sequential ordered mechanism, and the characterization of novel polymerases is often based on this premise (*9–15*). While this assumption is valid for DNA polymerases that exhibit high processivity, low to moderately processive DNA polymerases could, in principle, deviate from this strict "DNA-first" binding order. Recent discoveries of several DNA polymerases with novel properties such as low fidelity, a preference for certain dNTPs, selectivity for certain base pairs, and the use of damaged/unnatural substrates (*14, 16–21*) demand further investigations into their order of substrate binding.

DNA polymerase X (Pol X) from African swine fever virus (ASFV) is the smallest known DNA polymerase with 174 amino acid residues and a size of 20.3 kDa (*22*). Pol X is a very low fidelity polymerase and, most notably, catalyzes the incorporation of the dG:dGTP mismatch as efficiently as the dG:dCTP match (*21, 23*). Pol X also possesses moderate lesion bypass capabilities (*18*). On the basis of its

† This work was supported by NIH Grant GM43268. S.K. was partially supported by a Preston G. Hoff Fellowship.

* To whom correspondence should be addressed: Genomics Research Center, Academia Sinica, Taipei 115, Taiwan. Telephone: +886-2-2789-9930. Fax: +886-2-2789-9931. E-mail: tsai@chemistry.ohio-state.edu.

‡ The Ohio State University.

§ Academia Sinica.

[1] Abbreviations: ASFV, African swine fever virus; Pol, DNA polymerase; 2-AP, 2′-deoxy-2-aminopurine; 2-AP-dNTP, 2-aminopurine-2′-deoxyribose 5′-triphosphate; ddGTP, 2′,3′-dideoxyguanosine 5′-triphosphate; BSA, bovine serum albumin.

10.1021/bi800731m CCC: $40.75
Published on Web 07/04/2008

catalytic properties, Pol X has been implicated in mutagenic DNA repair and the viral hypermutagenicity (*21, 23, 24*). Pol X belongs to the X superfamily of nucleotidyltransferases (*22, 25*) and shares sequence and structural homology with mammalian Pol β but lacks the lyase domain and the N-terminal portion of the polymerase domain of the latter. Despite the lack of these structural elements, which are responsible for DNA binding in Pol β, Pol X is able to bind DNA with a very high affinity (*26*), largely due to its unique binding mode where it uses helix αE in the fingers subdomain, helix αC in the palm subdomain, and the interface of the palm and fingers subdomains to bind DNA (M.-I. Su et al., unpublished results; *26, 27*). Pol X has also been shown to be a highly distributive enzyme (*22*), unlike Pol β, which has been shown to be processive on short gapped DNA substrates owing to the presence of its 8 kDa lyase domain. A recent study using a quantitative fluorescence titration technique showed that Pol X binds gapped DNA in two distinct modes: one utilizing the total DNA binding site of Pol X and the other utilizing only the auxiliary DNA binding site where the enzyme binds to the double-stranded region of the DNA (*28*).

NMR structural analyses of free Pol X have shown that it can bind dNTPs with high affinity in the presence of Mg^{2+} (*27*). Notably, binding of the purine nucleotides (Mg^{2+}•dATP and Mg^{2+}•dGTP) induces extensive ^{1}H and ^{15}N chemical shift perturbations, propagating in both the finger and palm subdomains of Pol X (*27*). Further, modeling based on chemical shift perturbations suggested a conformational adjustment of subdomains upon Mg^{2+}•dNTP binding; such rearrangements have not been observed for other polymerases in the absence of DNA (*27*). Even though these studies suggested that free Pol X can bind Mg^{2+}•dNTP in its active site, it was not clear whether this binding is productive.

While all the DNA polymerases investigated to date seem to follow a sequential ordered mechanism, several related enzymes from the Pol X superfamily of nucleotidyltransferases have been shown to possess a sequential random mechanism (*29–32*). This suggests that the sequential ordered mechanism is not conserved throughout the nucleotidyltransferase superfamily. Further, this mechanism may not be required for nonprocessive DNA polymerases, lesion bypass DNA polymerases, and/or template-independent transferases.

In this study, we have used a classical steady-state kinetics approach to determine the kinetic mechanism of DNA and dNTP substrate binding to ASFV Pol X. Then we utilized substrate-trapping assays under pre-steady-state conditions to address the question of whether DNA or dNTP binding by Pol X results in a productive binary complex. Finally, using stopped-flow fluorescence technique, we analyzed the kinetics of DNA and dNTP binding by Pol X and the effect of substrate mixing order on the fluorescence transitions upon formation of the Pol X•DNA•dNTP ternary complex. Results of our kinetic analyses suggest that the order of substrate binding by ASFV Pol X differs from the bi-bi ordered mechanism suggested for other DNA polymerases.

MATERIALS AND METHODS

Materials. Ultrapure dNTPs and G-25 Microspin columns were purchased from GE Healthcare. [γ-^{32}P]ATP was purchased from MP Biomedicals. T4 polynucleotide kinase was obtained from New England BioLabs. BSA was from Roche. Reverse phase C18 cartridges were from Waters Corp. Materials and reagents not listed here were of standard molecular biology grade.

Purification of Enzymes. Recombinant ASFV Pol X was expressed and purified as previously described (*21*). The H115W mutant was generated by site-directed mutagenesis with forward primer 5′-GAGGAAAAACCATACG-CAATATTTTGGTTTACGGGTCCCGTTTC-3′ and reverse primer 5′-GAAACGGGACCCGTAAACCAAAATATTGC-GTATGGTTTTTCCTC-3′ using the QuikChange method (Stratagene). Successful mutagenesis was verified by sequencing of the plasmid. The mutant enzyme was expressed and purified as described for wild-type (WT) Pol X. The enzyme concentrations were determined by UV absorbance at 280 nm using extinction coefficients of 15930 and 21430 M^{-1} cm^{-1} for Pol X and the H115W mutant, respectively. The enzymes appeared to be homogeneous on the basis of SDS−PAGE developed using the silver staining method.

DNA Substrates. The sequences of DNA substrates used in this study are listed in Table 1. Custom synthesized oligomers were purchased from Integrated DNA Technologies (Coralville, IA). Each DNA oligomer was further purified with polyacrylamide−urea denaturing gels and extracted with 500 mM ammonium acetate and 1 mM EDTA. Extracted oligomers were subsequently desalted on a Sep-Pak C18 cartridge and eluted using a methanol/water mixture (60:40). After the solvent had been removed with a vacuum, the oligomers were resuspended in TE buffer [10 mM Tris-HCl and 0.1 mM EDTA (pH 8.0)], and the concentration was determined by UV using extinction coefficients provided by the vendor. The oligomers were then stored at −20 °C.

DNA substrates used in the chemical quench experiments were 5′-end-labeled using T4 polynucleotide kinase and [γ-^{32}P]ATP (4500 Ci/mol) according to the manufacturer's protocol. The T4 polynucleotide kinase was inactivated by heating the solution at 65 °C for 20 min. The labeled primer was separated from unreacted ATP using a G-25 microspin column. Typically, only 5% of the substrate molecules were labeled with ^{32}P. All DNA substrates were assembled at room temperature by mixing primer, template, and downstream oligomers in a 1:1.1:1.2 molar ratio. Once assembled, substrates were stored at 4 °C prior to use.

Steady-State Inhibition Assays. Steady-state reactions were initiated by manually adding 0.3 nM Pol X to a reaction mixture containing 100 nM DNA substrate (or varied from 5 to 200 nM), 500 μM dNTP (or varied from 10 to 500 μM), and the appropriate concentration of inhibitor in a reaction buffer containing 140 mM KCl, 50 mM tris-borate, 3% glycerol, 10 mM $MgCl_2$, 100 μg/mL BSA, and 1 mM DTT (pH 7.5) at 37 °C. All concentrations listed above are postmixing. Aliquots (10 μL) of the reaction mixture were subsequently quenched by being mixed with 10 μL of formamide at time points ranging from 15 s to 60 min. Elongated DNA product in the quenched reactions was separated from the substrate DNA using 19% denaturing polyacrylamide gels. Formation of the pyrophosphate product was not monitored. Gel visualization was conducted by phosphor screen autoradiography using a STORM840 scanner from GE Healthcare. Band intensity quantitation and data plotting were performed using ImageQuant (GE Healthcare) and SigmaPlot 9.0 (Systat Software Inc.), respectively. DNA

Table 1: DNA Substrates

Designation[a]	Sequence[b]	Assay to be used in
45(G)	5′-^{32}P-GCCTCGCAGCCGTCCAACCAACTCA GCTCGATCCAATGCCGTCC 3′-CGGAGCGTCGGCAGGTTGGTTGAGT**G**CGAGCTAGGTTACGGCAGG	Substrate in steady-state and DNA-trapping assay
45(T)	5′-^{32}P-GCCTCGCAGCCGTCCAACCAACTCA GCTCGATCCAATGCCGTCC 3′-CGGAGCGTCGGCAGGTTGGTTGAGT**T**CGAGCTAGGTTACGGCAGG	Substrate in steady-state assays
35dd(G)	5′-GCCTCGCAGCCGTCCAAC[d] AAGTCACCTCAATCCA 3′-CGGAGCGTCGGCAGGTTG**G**TTCAGTGGAGTTAGGT	Inhibitor in steady-state assays
35(G)	5′-GCCTCGCAGCCGTCCAAC AAGTCACCTCAATCCA 3′-CGGAGCGTCGGCAGGTTG**G**TTCAGTGGAGTTAGGT	Non-labeled DNA in DNA-trapping assay
35(CG)	5′-^{32}P-GCCTCGCAGCCGTCCAA AAGTCACCTCAATCCA 3′-CGGAGCGTCGGCAGGTT**CG**TTCAGTGGAGTTAGGT	Nucleotide-trapping assay
36dd(T)	5′-GCCTCGCAGCCGTCCAACC[d] AGTCACCTCAATCCA 3′-CGGAGCGTCGGCAGGTTGG**T**ATCAGTGGAGTTAGGT	2-AP-dNTP fluorescence assays
18dd/35AP	5′-GCCTCGCAGCCGTCCAAC[d] 3′-CGGAGCGTCGGCAGGTTG**G**ÃTCAGTGGAGTTAGGT	2-AP-DNA fluorescence assays
35dd(GÃ)	5′-GCCTCGCAGCCGTCCAAC[d] AGTCACCTCAATCCA 3′-CGGAGCGTCGGCAGGTTG**G**ÃTCAGTGGAGTTAGGT	DNA binding fluorescence assays

[a] Substrates with the dd designation have a dideoxy-terminated primer terminus. The number in designation is the total number of bases in the template. The templating base in the gap is shown in parentheses. [b] In the gapped DNA substrates, the downstream oligonucleotide is 5′-phosphorylated. Ã refers to a 2-aminopurine base. C[d] represents 2′,3′-dideoxycytidine 5′-monophosphate.

product formation as a function of time was fit using linear regression to obtain the steady-state rate, V_{obs}. V_{obs}, as a function of varied substrate concentration, was then fit to the hyperbolic equation $V_{obs} = V_{max}[S]/(K_m + [S])$, where [S] is the concentration of the varied substrate, to obtain steady-state kinetic parameters V_{max} (maximum rate) and K_m (Michaelis constant). V_{obs} values obtained for each inhibitor−varied substrate pair were also fit globally to determine the type of inhibition and inhibition parameters using the following equations.

$$V_{obs} = \frac{V_{max}[S]}{K_m\left(1 + \frac{[I]}{K_I}\right) + [S]} \quad \text{(competitive inhibition)}$$

$$V_{obs} = \frac{V_{max}[S]}{K_m + [S]\left(1 + \frac{[I]}{K_{II}}\right)} \quad \text{(uncompetitive inhibition)}$$

$$V_{obs} = \frac{V_{max}[S]}{K_m\left(1 + \frac{[I]}{K_I}\right) + [S]\left(1 + \frac{[I]}{K_{II}}\right)} \quad \text{(noncompetitive inhibition)}$$

where the inhibition constant, K_I, describes inhibitor binding to E alone and K_{II} describes inhibitor binding to the E•S complex.

DNA-Trapping Assay. Solution A containing 400 nM Pol X and 400 nM 45(G) DNA substrate [labeled with ^{32}P (Table 1)] was rapidly mixed with solution B containing 1 mM dCTP and 4 μM 35(G) nonlabeled DNA in a 1:1 ratio in reaction buffer containing 140 mM KCl, 50 mM tris-borate, 3% glycerol, 10 mM $MgCl_2$, 100 μg/mL BSA, and 1 mM DTT (pH 7.5) at 37 °C using a rapid chemical quench instrument (KinTek Instrument Corp., State College, PA). Reactions were quenched with 0.6 M EDTA at incremental time points ranging from 1 to 150 s. In the control experiments, either nonlabeled DNA was not present (control 1), or both labeled 45(G) and nonlabeled 35(G) DNA were in solution B (control 2). Product formation was visualized and analyzed as described above. Product formation as a function of time for control 1 was fit to the single-exponential equation $[DNA_{n+1}] = A(1 - e^{-kt})$, where A and k represent the amplitude and the observed rate constant of single-nucleotide incorporation, respectively. Product formation in presence of nonlabeled DNA was fit to the "burst" equation $[DNA_{n+1}] = A(1 - e^{-kt}) + V_{ss}t$, where A, k, and V_{ss} represent the burst amplitude, pre-steady-state rate constant, and steady-state rate, respectively.

Nucleotide-Trapping Assay. This assay was performed in a manner similar to that of the DNA-trapping assay except that the reactions were quenched manually with formamide. Solution A contained 450 nM Pol X and 100 μM ddGTP, whereas solution B contained 200 nM 35(CG) DNA substrate, 1 mM dGTP, and 1 mM dCTP. In the control reaction, ddGTP was added to solution B and not to solution A. One nucleotide extension of the DNA substrate (incorporation of ddGTP and dGTP) as a function of time was fit to the double-exponential equation $[DNA_{n+1}] = A_1e^{-k_1t} + A_2e^{-k_2t} + C$, where k_1 and k_2 are rate constants of the first and second incorporations, respectively, and C is the concentration of the dd-terminated DNA product.

Stopped-Flow Fluorescence Assays. Stopped-flow experiments were performed on an Applied Photophysics SX 18MV stopped-flow apparatus. For the 2-aminopurine (2-AP) fluorescence assays, the excitation wavelength was 312 nm with a spectral bandpass of 4 nm. 2-AP emission was monitored using a 360 nm high pass filter (Corion). For tryptophan (Trp) fluorescence experiments, the excitation wavelength was 290 nm with a spectral bandpass of 4 nm. Trp emission was monitored using a 335 nm high pass filter except that a 335−345 nm bandpass filter was used when 2-AP fluorophore was also present in the reaction mixture. All the reactions were performed in an assay buffer containing 140 mM KCl, 50 mM tris-borate, 3% glycerol, 10 mM $MgCl_2$, and 1 mM DTT (pH 7.5) at 37 °C. Typically, a minimum of seven runs were performed for each reaction and the traces averaged. The averaged traces were fit using

Applied Photophysics software to either a single- or double-exponential equation:

$$\text{fluorescence} = Ae^{-kt} + C$$

$$\text{fluorescence} = A_1e^{-k_1t} + A_2e^{-k_2t} + C$$

where k_1 and k_2 are rate constants of fluorescence change, A_1 and A_2 are the respective amplitudes, and C is an offset constant.

RESULTS

Steady-state kinetics is often employed to understand the enzyme mechanism of bisubstrate reactions, and dead-end inhibition patterns are generally the most informative in distinguishing different mechanisms of substrate binding. Here we have used DNA and nucleotide substrate analogues in Pol X-catalyzed steady-state reactions to elucidate the preferred order of substrate binding for this enzyme.

Inhibition Patterns Using DNA Substrate Analogue ddDNA. DNA with a 3′-dideoxy-terminated primer (ddDNA) is a substrate analogue that is commonly used in the mechanistic and structural studies of DNA polymerases because the latter can bind ddDNA with an affinity similar to that for unmodified DNA and undergo any necessary conformational change but cannot catalyze the chemical step, resulting in dead-end inhibition (*33*). A 35dd(G) DNA substrate analogue (Table 1) was used as an inhibitor during Pol X-catalyzed incorporation of dCTP into 45(G) DNA under steady-state conditions. Note that the templating base in both the 45(G) DNA substrate and inhibitor is guanine which forms a Watson−Crick base pair with incoming dCTP. In a typical set of inhibition assays, the initial rate of product formation (V_{obs}) was measured as a function of varied substrate concentration in the presence of incremental amounts of the inhibitor. A representative example of reaction time courses is shown in Figure 1A, and a set of hyperbolic fits of V_{obs} versus varied substrate concentration is presented in Figure 1B. Kinetic constants V_{max} and K_m obtained from the concentration dependence of the initial rate of product formation are summarized in Table 2.

When DNA was the varied substrate, the double-reciprocal plot exhibited a set of lines with a common intercept but increasing slopes at increasing inhibitor concentrations (Figure 1C), the characteristic pattern of competitive inhibition. A global fit of the entire data set to a competitive inhibition kinetic model yielded an inhibition constant K_I of 0.0064 μM (Table 2).

When the dCTP substrate was varied, the 35dd(G) DNA substrate analogue behaved as an uncompetitive inhibitor as reflected by the double-reciprocal plot which exhibited a set of parallel lines (Figure 1D). Global fitting showed that the corresponding data set fits best to the uncompetitive inhibition kinetic model with a K_{II} of 0.21 μM. Global fitting to different kinetic models, along with respective R^2 values, is shown in Figure S1 of the Supporting Information. The uncompetitive inhibition versus nucleotide substrate suggests that the dideoxy-terminated DNA substrate analogue binds to the Pol X·dCTP binary complex and not to the free enzyme. If this DNA analogue also bound to the free Pol X, the pattern of inhibition would be expected to be noncompetitive. This in turn implies that dCTP is the leading substrate and that, unlike other DNA polymerases, Pol X does not always bind to the DNA substrate first.

Inhibition Patterns Using a ddDNA Substrate Analogue with a Mismatch at the Templating Position. An essential feature of the ordered sequential mechanism is that the first substrate binding creates a binding site for the second substrate. Accordingly, the ddDNA substrate analogue with a mismatch at the templating position would have a lower affinity for the Pol X·dNTP binary complex and act as a poor inhibitor. We used 35dd(G) DNA as an inhibitor in Pol X-catalyzed incorporation of dATP into 45(T) DNA under steady-state conditions. As expected, the 35dd(G) DNA substrate analogue demonstrated competitive inhibition toward the 45(T) DNA substrate with a significantly higher K_I (0.46 μM). The double-reciprocal plot when dATP was the varied substrate (Figure 1E) showed both the slope and the intercept effect. Consistently, the global analysis of the data suggested noncompetitive inhibition with K_I and K_{II} values of 0.29 and 0.84 μM, respectively, implying that the inhibitor binds to both the free Pol X and the Pol X·dATP complex. The fact that the same 35dd(G) DNA exhibited uncompetitive inhibition versus the varied dCTP substrate suggests that in the presence of matched dNTP the inhibitor binds primarily to the Pol X·dNTP complex utilizing a dNTP-directed DNA binding site. The noncompetitive pattern of inhibition in the absence of matched dNTP can be explained by the existence of an alternative Pol X−DNA binding mode which is independent of dNTP binding.

Inhibition by Pyrophosphate. Pyrophosphate (PP_i) is a product of the polymerase reaction and has been previously used as an inhibitor in mechanistic studies of DNA polymerases (*1, 4, 29, 30*). We attempted to use PP_i inhibition in steady-state assays to gain further insights into the Pol X mechanism. However, we found that Pol X is not inhibited noticeably by up to 1 mM PP_i. At higher PP_i concentrations, there was modest inhibition (data not shown); however, quantitative analysis of inhibition was not possible because of PP_i solubility restrictions.

Inhibition Patterns Using a Mismatch Nucleotide. Previous kinetic studies have shown that Pol X displays a very high binding affinity for purine:purine mismatches under pre-steady-state conditions (*21*). Specifically, for a dG:dATP (template:incoming nucleotide) mismatch, Pol X displays tight binding ($K_{D,app}$ = 80 μM) but a very slow turnover rate (430-fold slower than the rate of correct dG:dCTP incorporation). Accordingly, it is expected that dATP can act as an effective inhibitor in Pol X-catalyzed incorporation of dCTP into 45(G) DNA.

Using dATP as an inhibitor and dCTP as a varied substrate, the pattern of inhibition was competitive with a K_I of 48 μM. There was no detectable incorporation under the steady-state conditions when dATP was used as the substrate in the absence of dCTP. These results confirmed that dATP can be used as a dCTP analogue in Pol X inhibition studies addressing the order of substrate binding.

The effect of incremental amounts of dATP on initial velocity, with DNA as the varied substrate, is shown in Figure 1F. If DNA were the leading substrate, dATP would exhibit uncompetitive inhibition toward DNA. However, the double-reciprocal plot exhibited the slope and intercept effect (Figure 1F), and the global regression fit best to a noncompetitive inhibition model with K_I and K_{II} values of 150 and

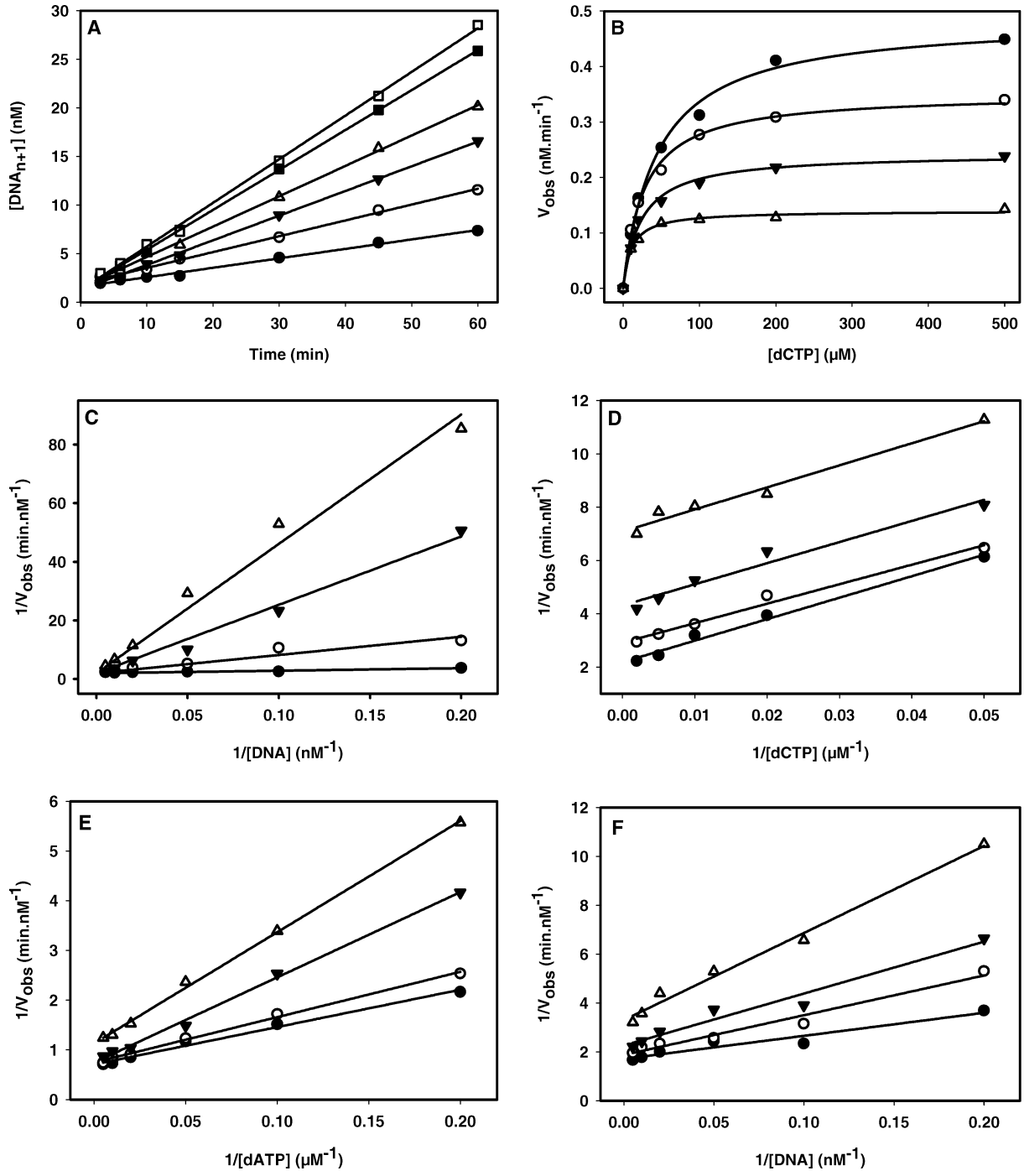

FIGURE 1: Inhibition by ddDNA and mismatch dNTP in Pol X-catalyzed steady-state reactions. The concentrations used in the following reactions were 0.3 nM Pol X, 100 nM DNA substrate (or varied), and 500 μM dNTP substrate (or varied). All concentrations are after mixing. (A) Incorporation of dCTP into 45(G) DNA in the absence of inhibitor. dCTP concentrations were 10 (●), 20 (○), 50 (▼), 100 (△), 200 (■), and 500 μM (□). The data were fit using linear regression to obtain V_{obs}. (B) dCTP concentration dependence of V_{obs}, obtained as described for panel A, in the presence of the following 35dd(G) inhibitor concentrations: 0 (●), 50 (○), 200 (▼), and 500 nM (△). V_{obs} values as a function of dCTP concentration were fit to a hyperbolic equation to provide k_{max} and K_m values listed in Table 2. (C) Double-reciprocal plots for assays with a constant dCTP concentration and varied 45(G) DNA substrate concentrations in the presence of 0 (●), 50 (○), 200 (▼), and 500 nM (△) 35dd(G) DNA inhibitor. (D) Double-reciprocal plots for assays with a constant 45(G) DNA concentration and varied dCTP substrate concentrations in the presence of 0 (●), 50 (○), 200 (▼), and 500 nM (△) 35dd(G) inhibitor. (E) Double-reciprocal plots for assays with a constant 45(T) DNA concentration and varied dATP substrate concentrations in the presence of 0 (●), 50 (○), 200 (▼), and 500 nM (△) 35dd(G) inhibitor with a noncomplementary templating base. (F) Double-reciprocal plots for assays with a constant dCTP concentration and varied 45(G) DNA substrate concentrations in the presence of 0 (●), 50 (○), 200 (▼), and 500 μM dATP (△).

640 μM, respectively. This result provides strong evidence against the order of substrate binding proposed for other DNA polymerases, where DNA always binds before dNTP binding.

DNA-Trapping Assay under Pre-Steady-State Conditions. Substrate trapping is another common method used to understand enzyme mechanisms. DNA trapping has been used previously by researchers to establish the kinetic

Table 2: Kinetic Parameters for Substrate Inhibition in Pol X-Catalyzed Steady-State Reactions

varied substrate	nonvaried substrate	inhibitor	V_{max} (nmol/min)	K_m (μM)	type of Inhibition[a]	global fitting[b] V_{max} (nmol/min)	global fitting[b] K_m (μM)	global fitting[b] K_I (μM)	global fitting[b] K_{II} (μM)
dCTP	45(G)	none	0.49 ± 0.02	45 ± 5	UC	0.47	41		0.21
		50 nM 35dd(G)	0.35 ± 0.02	27 ± 2					
		200 nM 35dd(G)	0.24 ± 0.01	23 ± 3					
		500 nM 35dd(G)	0.14 ± 0.01	10 ± 1					
45(G)	dCTP	none	0.46 ± 0.01	0.003 ± 0.001	C	0.45	0.0029	0.0064	
		50 nM 35dd(G)	0.43 ± 0.02	0.029 ± 0.004					
		200 nM 35dd(G)	0.45 ± 0.03	0.090 ± 0.012					
		500 nM 35dd(G)	0.42 ± 0.08	0.182 ± 0.051					
dATP	45(T)	none	1.5 ± 0.03	13 ± 2	NC	1.51	13	0.29	0.84
		50 nM 35dd(G)	1.4 ± 0.04	14 ± 2					
		200 nM 35dd(G)	1.3 ± 0.04	19 ± 3					
		500 nM 35dd(G)	0.91 ± 0.02	21 ± 2					
45(T)	dATP	none	1.9 ± 0.06	0.030 ± 0.003	C	1.88	0.030	0.46	
		50 nM 35dd(G)	1.9 ± 0.04	0.035 ± 0.002					
		200 nM 35dd(G)	1.9 ± 0.09	0.043 ± 0.006					
		500 nM 35dd(G)	1.7 ± 0.09	0.075 ± 0.009					
dCTP	45(G)	none	0.52 ± 0.02	32 ± 5	C	0.51	35	48	
		20 μM dATP	0.49 ± 0.02	55 ± 7					
		200 μM dATP	0.56 ± 0.02	125 ± 13					
		500 μM dATP	0.44 ± 0.05	299 ± 66					
45(G)	dCTP	none	0.59 ± 0.03	0.006 ± 0.001	NC	0.57	0.0056	150	640
		50 μM dATP	0.51 ± 0.02	0.007 ± 0.001					
		200 μM dATP	0.45 ± 0.02	0.010 ± 0.002					
		500 μM dATP	0.31 ± 0.01	0.012 ± 0.002					

[a] C, UC, and NC refer to competitive, uncompetitive, and noncompetitive inhibition patterns, respectively. [b] Errors associated with global fitting are listed in Table S1 of the Supporting Information.

mechanism for several DNA polymerases (*8, 34*). In these assays, the labeled DNA substrate is incubated with the polymerase and is then mixed with an excess of nonlabeled DNA and the correct nucleotide substrate. If the polymerase binds DNA first in a productive manner, there should not be a significant decrease in the burst amplitude of product formation when it is challenged with nonlabeled DNA. On the other hand, if DNA binding is nonproductive and DNA dissociation is required prior to formation of a productive complex, an excess of nonlabeled DNA should effectively compete for the enzyme active sites, resulting in a smaller burst amplitude.

We performed a DNA-trapping assay in which Pol X preincubated with labeled 45(G) DNA was mixed with dCTP and a 10-fold excess of nonlabeled 35(G) DNA. The final concentrations after mixing were as follows: 200 nM Pol X, 200 nM labeled 45(G) DNA, 2 μM nonlabeled 35(G) DNA, and 500 μM dCTP. It is important to note that Pol X binds DNA with a high affinity (K_d^{DNA} in the low nanomolar range; see ref *26* and this report); therefore, most of the labeled 45(G) DNA should be in the Pol X·DNA binary complex. The product formation exhibited burst kinetics with an amplitude of 44 ± 3 nM (Figure 2), which is ~3-fold smaller than the burst amplitude in the control experiment from which nonlabeled DNA was omitted. In the second control experiment, where labeled DNA was mixed with nonlabeled DNA, the burst amplitude was 11 ± 3 nM, which closely corresponds to the percentage of labeled 45(G) DNA in the total DNA pool. These results suggest that a large fraction of the preincubated DNA dissociates from the preformed Pol X·DNA binary complex before nucleotide incorporation. This implies that either dissociation of DNA from the Pol X·DNA complex is much faster than binding of dNTP to the Pol X·DNA complex or the preformed binary complex is nonproductive and Pol X binds DNA in a productive manner only after binding to dNTP. Trapping of one-third

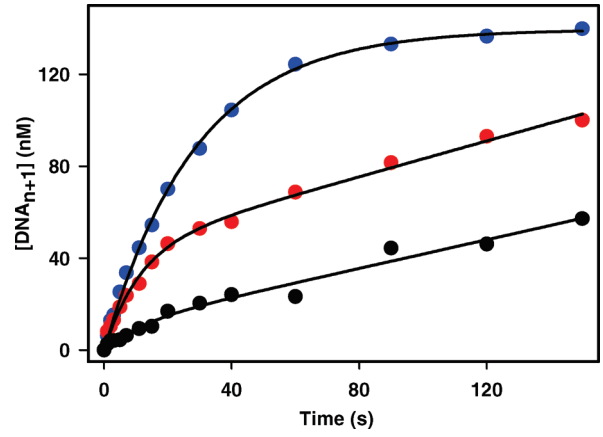

FIGURE 2: DNA-trapping experiment under pre-steady-state conditions. Product formation as a function of time when solution A, containing 200 μM 45(G) DNA substrate and 200 μM Pol X, was mixed with solution B, containing 500 μM dCTP (all concentrations are after mixing), exhibits single-exponential kinetics with an amplitude 140 ± 1 nM and a rate of 0.035 ± 0.001 s^{-1} (blue). Product formation when solution A, containing Pol X and 45(G) DNA, was mixed with solution B, containing dCTP and a 10-fold excess of nonlabeled 35(G) DNA, exhibits burst kinetics with a burst amplitude of 44 ± 3 nM, a burst rate constant of 0.091 ± 0.010 s^{-1}, and a steady-state rate of 0.39 ± 0.03 nM/s (red). A control experiment in which solution A, containing Pol X alone, was mixed with solution B, containing dCTP and both labeled 45(G) and nonlabeled 35(G) DNA, results in burst kinetics with an amplitude of 11 ± 3 nM, a burst rate constant of 0.086 ± 0.051 s^{-1}, and a steady-state rate of 0.31 ± 0.03 nM/s (black).

of the DNA suggests that even though free Pol X might bind DNA in a nonproductive manner, dNTP binding to the binary Pol X·DNA binary complex induces DNA rearrangement without its dissociation from the enzyme.

Nucleotide-Trapping Assay under Pre-Steady-State Conditions. To establish whether dNTP can bind to Pol X in a productive manner and become incorporated into the DNA

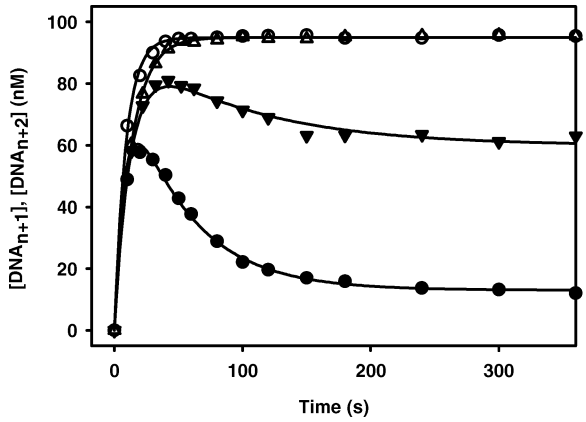

FIGURE 3: Nucleotide-trapping experiment under pre-steady-state conditions. Triangles represent data for a reaction that was initiated by mixing of solution A, containing 225 nM Pol X and 50 μM ddGTP, with solution B, containing two-nucleotide gapped 35(CG) DNA substrate (100 nM), 500 μM dGTP, and 500 μM dCTP (all concentrations are after mixing). In the control reaction (circles), ddGTP was added to solution B instead of solution A. Total (DNA$_{n+1}$ + DNA$_{n+2}$) product formation (△) shows similar kinetics as the control (○); however, accumulation of the DNA$_{n+1}$ product was significantly higher (63 ± 2 nM) in the first reaction (▼) compared to the control (●), where only 14 ± 1 nM DNA$_{n+1}$ product accumulated.

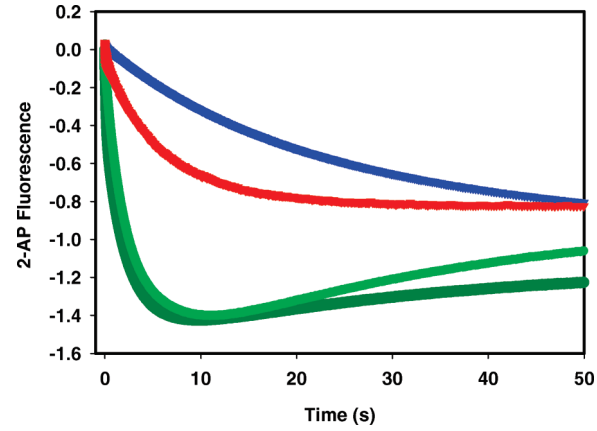

FIGURE 4: Effect of substrate mixing order in stopped-flow assays using 2-AP-dNTP. Fluorescence change upon binding of 2-AP-dNTP to Pol X (red trace), binding of 2-AP-dNTP to the Pol X•DNA binary complex (blue trace), and binding of DNA to the Pol X•2-AP-dNTP binary complex (green trace). Concentrations used in all reactions were as follows: 2 μM Pol X, 2 μM 36dd(T) DNA, and 2 μM 2-AP-dNTP. The fast phase in the green trace may correspond to DNA binding to the Pol X•2-AP-dNTP binary complex or conformational rearrangements in the Pol X•DNA•2-AP-dNTP ternary complex. The slow fluorescence increase (second phase in the green trace) could be caused by release of 2-AP-dNTP from the Pol X•DNA•2-AP-dNTP ternary complex due to weaker binding affinity of dNTP. This assignment is supported by a decrease in the amplitude of this phase when all the substrate concentrations are increased to 5 μM (dark green trace).

substrate without first dissociating, we performed a dNTP-trapping assay similar to the DNA-trapping assay described above. In this experiment, we utilized the ability of Pol X to incorporate 2′,3′-dideoxyguanosine 5′-triphosphate (ddGTP) with an efficiency similar to that for unmodified dGTP (data not shown). Incorporation of ddGTP into 35(CG) DNA (two-nucleotide gap DNA with 5′-CG templating bases) leads to chain termination, thus preventing incorporation of the second nucleotide (dCTP), which in turn results in accumulation of the DNA$_{n+1}$ product.

In the nucleotide-trapping assay, Pol X, preincubated with 50 μM ddGTP, was mixed with 100 nM 35(CG) DNA, 500 μM dGTP (competing nucleotide), and 500 μM dCTP (nucleotide for the second incorporation). All concentrations listed above are postmixing. For the control reaction, ddGTP was mixed with dGTP instead of being preincubated with Pol X. If Pol X were not able to bind ddGTP tightly or bound it in a nonproductive manner, then the excess of dGTP would dilute ddGTP, thus preventing ddGTP incorporation and chain termination, and the results of the nucleotide-trapping and control assays would be identical. However, when Pol X was preincubated with ddGTP, 63 ± 2 nM DNA$_{n+1}$ product accumulated compared to the accumulation of 14 ± 1 nM for the control reaction (Figure 3). Less than 100% chain termination can possibly be explained by the fact that ddGTP concentration was not sufficiently high to saturate all Pol X active sites. The amplitude and the rate of the first turnover (measured as total product formation versus time) remained unchanged in these two reactions. These results clearly show that dNTP can bind productively in the Pol X active site, and subsequent DNA binding results in nucleotide incorporation.

Varied Order of Substrate Mixing in Stopped-Flow Fluorescence Assays. To further elucidate the microscopic steps underlying the unusual substrate binding order of Pol X, we investigated Pol X reactions in stopped-flow assays. First, the effect of the varied order of substrate addition was examined using 2-aminopurine-2′-deoxyribose 5′-triphosphate (2-AP-dNTP), a fluorescent analogue of dATP. Addition of 2-AP-dNTP to Pol X resulted in a relatively fast fluorescence decay (Figure 4, red trace), while addition of 2-AP-dNTP to Pol X preincubated with 36dd(T) DNA produced a much slower fluorescence decay (Figure 4, blue trace), suggesting that dNTP binds to Pol X faster in the absence of DNA. We also measured the rate of dissociation of 2-AP-dNTP from the Pol X•2-AP-dNTP binary complex and the Pol X•2-AP-dNTP•ddDNA ternary complex as the rate of 2-AP fluorescence increase upon mixing of the preformed complexes with an excess of dATP (data not shown). In both cases, the rates were very similar. Together, the results suggest that Pol X has a weaker binding affinity for 2-AP-dNTP in the presence of DNA. When ddDNA was added to the Pol X•2-AP-dNTP complex, a fast fluorescence decay was observed (Figure 4, first phase in the green trace), suggesting that DNA binds to the Pol X•2-AP-dNTP complex at a rate much faster than the rate of binding of 2-AP-dNTP to the Pol X•DNA complex. Note that the slow fluorescence increase seen in the green trace is due to the release of 2-AP-dNTP because of the weaker binding affinity in presence of DNA, as described above. This is also supported by decrease in the relative amplitude of this phase when the concentration of all substrates is increased 2.5-fold (Figure 4, dark green trace). Taken together, these results suggest that the formation of the Pol X•DNA•2-AP-dNTP ternary complex would be faster if Pol X binds to the nucleotide first. Note that these data were obtained at equal concentrations of each substrate. However, for biological systems, the dNTP concentrations are expected to be much higher than the DNA concentration; under these conditions, we can surmise that the preference of Pol X for dNTP as the first substrate would be further increased.

Kinetics of Nucleotide Binding and Dissociation. To determine the kinetic parameters for Pol X−dNTP binding and dissociation, we created the H115W mutant containing a fluorescent Trp residue in the active site. WT Pol X also contains a Trp residue away from the active site, but it does not exhibit a significant fluorescence change upon nucleotide binding and incorporation (data not shown). We first compared the binding and dissociation of 2-AP-dNTP to Pol X and H115W utilizing the fluorescence signal from 2-AP. Both enzymes exhibited similar kinetics of 2-AP-dNTP binding and dissociation (Supporting Information, Figure S2A,B). Then we monitored the Trp fluorescence signal in response to 2-AP-dNTP binding. The rate of Trp fluorescence change was identical to that of the 2-AP fluorescence change of the nucleotide (Supporting Information, Figure S2C), implying that both the fluorescent probes respond to the same molecular process, namely, nucleotide binding. On the basis of the observations described above, kinetic parameters for nucleotide binding to H115W can be assumed to be similar to that for WT Pol X.

To calculate the bimolecular rate of nucleotide binding, 1 μM H115W was mixed with incremental amounts of one of four dNTPs, in the presence of 10 mM *free* Mg^{2+} in both solutions, and the rate of fluorescence change was measured and plotted as a function of nucleotide concentration (Figure 5A,B). The bimolecular rate of dNTP binding was calculated by pseudo-first-order approximation as the slope of this linear concentration dependence. We also investigated the dependence of dNTP binding to H115W on Mg^{2+} concentration. Our data suggest that the enzyme binds dNTP only in the form of Mg^{2+}•dNTP (Supporting Information, Figure S3). To measure the rate of nucleotide dissociation, H115W incubated with an excess of either dNTP was mixed with EDTA in a stopped-flow apparatus and the change in fluorescence was fit to a single-exponential equation (Figure 5C). The ability of EDTA to effect dNTP dissociation was comparable to that by addition of an excess of dNTP; when the H115W•2-AP-dNTP complex was mixed with excess dATP, dCTP, dGTP, dTTP, or EDTA, the fluorescence signal changed with similar rates of 0.048, 0.053, 0.048, 0.053, and 0.069 s^{-1}, respectively. Also, this rate was independent of the concentration of the binary complex as well as the excess dNTP concentration. Table 3 lists the kinetic parameters for binding and dissociation of each nucleotide with H115W and calculated K_d^{dNTP} values. Figure 5 and Table 3 clearly show that H115W, and Pol X by implication, can bind dNTP very tightly. Also noticeable is the fact that the purine nucleotides bind faster and dissociate slower than the pyrimidine nucleotides, resulting in a 10−25-fold lower K_d for the purines. K_d values for dGTP and dTTP determined in these studies are in an excellent agreement with the previously published data (*27*). For dCTP and dATP, there is small discrepancy in determined values: K_d^{dCTP} is somewhat larger than those previously published, whereas K_d^{dATP} is smaller.

Kinetics of Pol X−DNA Binding and Dissociation. Kinetics of DNA binding and dissociation were investigated using a 2-AP fluorescent probe in DNA [35dd(GÃ) (Table 1)] in stopped-flow assays. Binding of DNA to Pol X resulted in a fast increase in 2-AP fluorescence (Figure 6A). This fluorescence change can be best described by second-order binding kinetics with a k_{on} of 774 ± 30 μM^{-1} s^{-1}. To measure the rate of dissociation of the Pol X•DNA complex, Pol X was preincubated with a 2-AP-labeled DNA substrate and then rapidly mixed with a 10-fold excess of nonlabeled DNA. The observed fluorescence change exhibited single-exponential character with a k_{off} of 2.38 ± 0.04 s^{-1} (Figure 6B).

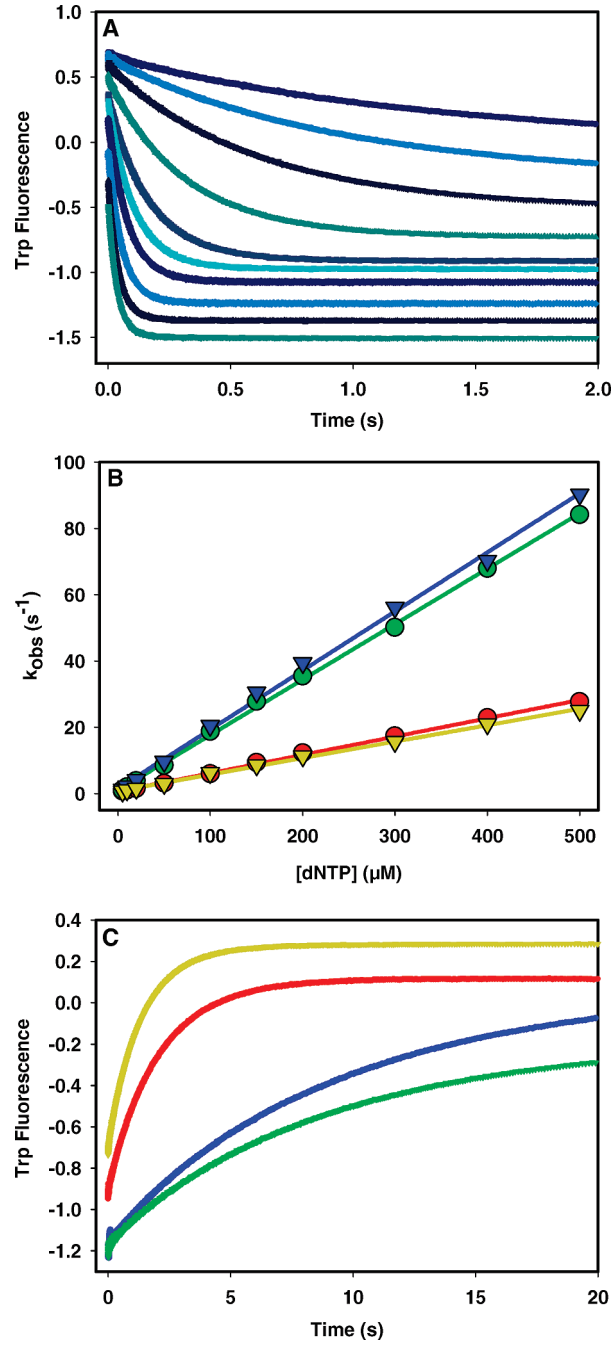

FIGURE 5: Kinetics of dNTP binding and dissociation in Trp fluorescence stopped-flow assays using the H115W mutant of Pol X. (A) Fluorescence changes upon rapid mixing of 1 μM H115W with dCTP at the following concentrations: 5, 10, 20, 50, 100, 150, 200, 300, 400, and 500 μM (from top to bottom; all concentrations are after mixing). The traces were fit to single-exponential equations to calculate k_{obs}. (B) k_{obs} as a function of dNTP concentration, obtained as described for panel A, for dATP (blue), dCTP (red), dGTP (green), and dTTP (yellow). Data were fit to a linear equation to obtain second-order dNTP binding rate constants, k_1^{dNTP}, listed in Table 3. (C) Fluorescence change upon addition of 20 mM EDTA to H115W•dNTP binary complexes. Fluorescence traces for dATP (blue), dCTP (red), dGTP (green), and dTTP (yellow) were fit to a single-exponential equation to obtain the dissociation rate constants, k_{-1}^{dNTP}, listed in Table 3.

Table 3: Kinetic Parameters for H115W−dNTP Binding

	k_1 ($\times 10^6$ M^{-1} s^{-1})	k_{-1} (s^{-1})	K_d (μM)[a]
dCTP	0.055 ± 0.001	0.51 ± 0.001	9.3 ± 0.2
dGTP	0.17 ± 0.002	0.12 ± 0.0004	0.71 ± 0.01
dATP	0.18 ± 0.003	0.11 ± 0.0005	0.61 ± 0.01
dTTP	0.050 ± 0.001	0.75 ± 0.002	15 ± 0.3

[a] k_1 was calculated as the slope of the linear fit of rate of dNTP binding as a function of dNTP concentration. k_{-1} was obtained from a single-exponential fit of the fluorescence change upon dNTP release in the presence of 20 mM EDTA. K_D was calculated as k_{-1}/k_1.

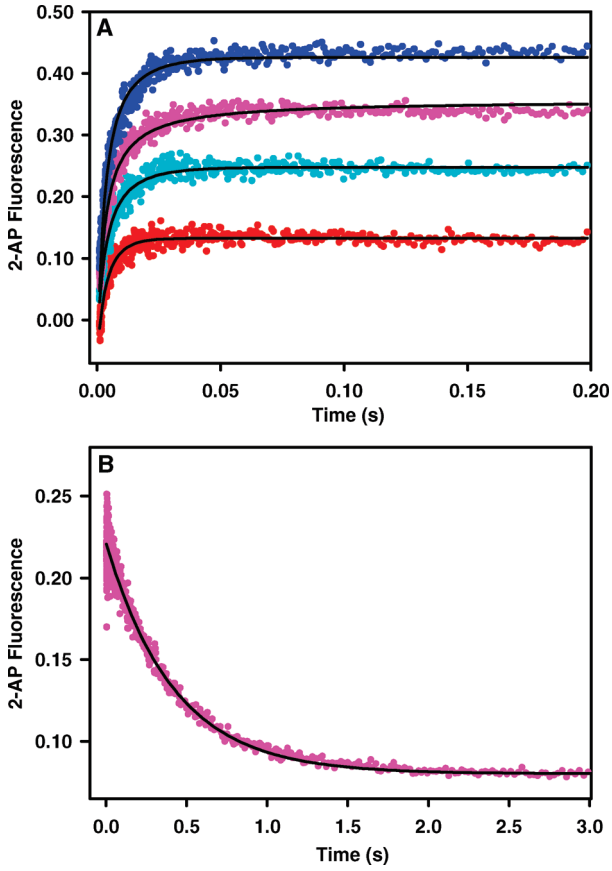

FIGURE 6: 2-AP fluorescence stopped-flow assays of Pol X−DNA binding and dissociation. (A) Fluorescence change upon rapid mixing of 400 nM 35dd(GĀ) DNA with Pol X at the following concentrations: 200 (red), 300 (cyan), 400 (pink), and 500 nM (blue). All concentrations are after mixing. The fluorescence traces fit best to the E + D → E·D kinetic model with second-order rate constants of 802 ± 29, 748 ± 25, 808 ± 27, and 740 ± 20 μM^{-1} s^{-1} for 200, 300, 400, and 500 nM Pol X, respectively. (B) Rapid mixing of preincubated 400 nM Pol X·DNA complex with a 10-fold excess of nonlabeled 45(G) DNA. Fitting data to a single-exponential equation yielded a DNA dissociation rate constant, k_{off}, of 2.4 ± 0.04 s^{-1}.

This rate was found to be independent of the concentration of enzyme or nonlabeled DNA, supporting the proposal that the observed fluorescence change corresponds to the Pol X·DNA dissociation step. The K_d^{DNA} value of 2.9 nM determined from kinetic data ($K_d^{DNA} = k_{off}/k_{on}$) correlates very well with the values of 3 nM obtained from an EMSA (*26*) but is somewhat higher than K_d values (0.017−1.5 nM) obtained from quantitative fluorescence studies (*28*).

Further Insights into Preferred Binding Order Provided by Stopped-Flow Fluorescence Assays with a 2-AP Probe in DNA Substrate. The effect of the order of substrate mixing was also investigated in stopped-flow assays using 18dd/35AP DNA (Table 1). Pol X readily accepts this DNA substrate, and the template−primer substrate with a 2-AP modification at the +1 templating position has been previously found to provide the best signal-to-noise ratio in stopped-flow fluorescence assays (*35, 36*). Addition of dCTP to the Pol X·ddDNA binary complex exhibited a slow fluorescence change with a single-exponential rate of 1.64 s^{-1} (blue trace in Figure 7A), whereas addition of DNA to a preformed Pol X·dCTP binary complex induced a much faster fluorescence change which fit to a double-exponential equation with rates of 79.3 and 9.92 s^{-1} (red trace in Figure 7A). These observations suggest that preceding dNTP binding facilitates following DNA binding and/or rearrangements that lead to a kinetically active ternary complex. To understand the reasons for a slower fluorescence change upon dNTP binding to a preformed Pol X·DNA binary complex,

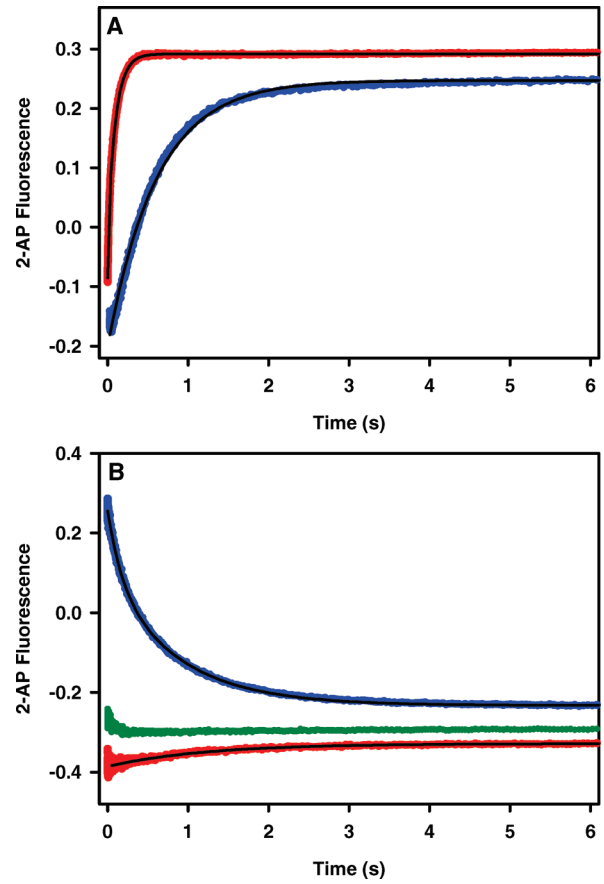

FIGURE 7: Effect of substrate mixing order in stopped-flow assays using a 2-AP-labeled DNA substrate. (A) The blue trace resulted from rapid mixing of solution A, containing 500 nM Pol X and 400 nM 18dd/35AP DNA, with solution B, containing 500 μM dCTP (all concentrations are after mixing). A single-exponential fit yielded a k of 1.64 ± 0.01 s^{-1}. The red trace represents rapid mixing of solution A, containing 500 nM Pol X and 500 μM dCTP, with solution B, containing 400 nM 18dd/35AP DNA. The fluorescence change fit a double-exponential equation with a k_1 of 79.3 ± 2.0 s^{-1} and a k_2 of 9.92 ± 0.06 s^{-1}. (B) Reactions were set up in a manner analogous to that for panel A, except dATP was used instead of dCTP. The blue trace (addition of dATP to the Pol X·DNA complex) fit a double-exponential equation with a k_1 of 5.92 ± 0.21 s^{-1} and a k_2 of 1.17 ± 0.02 s^{-1}. The red trace (addition of DNA to the Pol X·dATP complex) fit a single-exponential equation with a k of 0.831 ± 0.021 s^{-1}. The green trace shows data for rapid mixing of preincubated 500 nM Pol X, 400 nM 18dd/35AP DNA, and 500 mM dATP with a 10-fold excess of nonlabeled 45(G) DNA.

we analyzed the effect of dCTP concentration on the rate of this fluorescence change (Supporting Information, Figure S4A). We found that the rate increases linearly with an increase in dCTP concentration with a slope equal to 0.0023 μM^{-1} s^{-1} (Supporting Information, Figure S4B). Comparison of this value with the second-order rate constant for dCTP binding to free Pol X [0.055 μM^{-1} s^{-1} (Table 3)] implies that preceding DNA binding hinders subsequent nucleotide binding, which in turn results in the nucleotide binding being the rate-limiting step during the formation of the Pol X·DNA·dNTP ternary complex.

We then investigated how the presence of mismatched substrates would influence the appearance of stopped-flow fluorescence traces. Addition of 500 μM dATP to Pol X preincubated with 18dd/35AP DNA resulted in a fluorescence change in the direction opposite of that of the fluorescence change observed when dCTP was used (blue trace in Figure 7B). At the same time, addition of DNA substrate to Pol X preincubated with dATP did not produce a significant change in fluorescence intensity (red trace in Figure 7B). The small fluorescence increase might be attributed to the formation of a mismatched ternary complex or the formation of a small fraction of the Pol X·DNA binary complex. The latter suggestion is more plausible because it was found that the amplitude of the fluorescence change decreased at higher concentrations of dATP (data not shown). These results are consistent with the proposal that 18dd/35AP DNA with dG in a templating position cannot efficiently bind to the preformed Pol X·dATP binary complex. Accordingly, addition of dATP to the preformed Pol X·DNA complex induces DNA dissociation which results in a decrease in fluorescence (hence, the opposite direction of fluorescence change). This hypothesis is also consistent with the observation that the addition of a 10-fold molar excess of nonlabeled DNA to Pol X preincubated with dATP and 18dd/35AP DNA did not cause a significant fluorescence change, implying that most of the 2-AP-labeled DNA was in the unbound state (green trace in Figure 7B). Stopped-flow results are also in excellent agreement with the conclusion derived from the steady-state inhibition assays that the ddDNA substrate analogue with a mismatch at the templating position has a lower affinity for the Pol X·dNTP binary complex.

DISCUSSION

A number of DNA polymerases have been discovered in recent years. Accordingly, a number of structural and functional studies have been performed to improve our understanding of the mechanisms underlying their novel (and often unusual) properties (see refs *19* and *20* for reviews). For most of these DNA polymerases, kinetic analyses have been conducted using schemes and methodology developed earlier in classical studies of high-fidelity DNA polymerases (*37, 38*). For example, pre-steady-state kinetic experiments are generally designed with the assumption that the DNA polymerases initially form a binary complex with a DNA substrate and then bind a nucleotide substrate (*10–12, 15, 21*). The report presented here is the first analysis of the substrate binding order performed for a low-fidelity DNA polymerase. Our findings imply that different DNA polymerases might display different preferences for the order in which the two substrates bind.

In this study, we have employed classical approaches, such as steady-state inhibition assays and DNA-trapping assays, as well as novel experimental designs, for instance, use of dATP as an inhibitor and dNTP-trapping assays, to elucidate the order of DNA and dNTP substrate binding by Pol X. Our observations of uncompetitive inhibition by the ddDNA analogue when dNTP substrate was varied and noncompetitive inhibition by noncognate dNTP when the DNA substrate was varied are not consistent with the strictly ordered sequential mechanism with DNA as the first binding substrate. Our results can be interpreted only using a scheme in which dNTP binding is required for kinetically productive DNA binding. We should note that when the ddDNA analogue with a mismatch at the templating position was used, inhibition pattern deviated from uncompetitive behavior, implying that Pol X can bind DNA utilizing an alternative, dNTP-independent binding mode. Nevertheless, our results strongly suggest that dNTP is the preferred first substrate in the Pol X kinetic mechanism. These conclusions were also supported by substrate-trapping experiments under pre-steady-state conditions. Our results show that preincubated dNTP is preferably incorporated by Pol X, whereas Pol X·DNA trapping is not efficient. These data show that Pol X can bind a nucleotide substrate in a productive manner in the absence of DNA substrate, while DNA binding to Pol X, in the absence of dNTP, is mostly nonproductive. It suggests that, during the formation of a catalytically competent ternary complex, Pol X preferably binds DNA as the second substrate. Our proposed substrate binding order is also consistent with the highly distributive nature of polymerization by Pol X (*22*).

It is known that many DNA polymerases are able to bind dNTP in the absence of DNA substrate, forming a nonproductive E·dNTP binary complex. For example, X-ray structural studies of Klenow fragment of *E. coli* Pol I suggest that, in the absence of DNA substrate, the base and sugar moieties of bound dNTP adopt multiple conformations (*6*). Also, the structural analysis of mammalian Pol β revealed that dNTP binding interactions with this polymerase differ drastically between binary Pol β·dNTP and ternary Pol β·DNA·dNTP complexes (*7, 33*). While the incoming nucleotide makes a number of contacts with the active site residues in the ternary complex, the base of dNTP found in the crystal structure of the Pol β·dNTP binary complex does not interact with the active site and is directed toward residues from another asymmetric unit. The only structural moiety that remains similarly positioned in both the structures is γ-phosphate. NMR spectroscopy of methionine-labeled Pol β indicates that, in contrast to the observed global chemical shift perturbations upon formation of the Pol β·DNA·dNTP ternary complex, binding of dNTP alone does not cause global changes in the NMR spectra, suggesting that the enzyme structure remains largely unchanged. Interestingly, the increased complexity observed in these spectra may be attributed to the existence of multiple conformational states of the binary Pol β·dNTP complex (*39*).

The studies presented here show that Pol X binds dNTP very tightly and productively. Addressing the effect of DNA on the kinetics of dNTP binding and dissociation, we found that while the rate of dNTP dissociation was not affected by the presence of DNA, the rate of formation of the ternary complex was significantly reduced when Pol X was prein-

cubated with a DNA substrate. One possible explanation for this observation is that DNA binding by Pol X prior to dNTP binding brings the enzyme into a nonproductive conformation where subsequent nucleotide substrate binding is hindered or the rearrangement of the nonproductive ternary complex into its active conformation is retarded. On the other hand, preincubation of Pol X with a dNTP substrate might bring the enzyme into a conformation where productive DNA binding is facilitated while nonproductive DNA binding is prevented. This hypothesis is supported by the observation that the rate of DNA conformational rearrangement in the Pol X·DNA·dNTP ternary complex, as determined in 2-AP fluorescence stopped-flow assays, depends on the order of substrate mixing. In agreement with conclusions from our results, structural NMR studies of Pol X have shown that purine dNTP binding to the free enzyme induces large ^{1}H and ^{15}N chemical shift perturbations, which likely reflects a global change in Pol X conformation (*27*). It is important to note that nucleotide binding induces large chemical shift perturbations in residues in helices αC and αE, the proposed DNA-binding site in Pol X. It is plausible that nucleotide binding and the following conformational change create a binding site for the DNA substrate with a complementary templating base.

Most DNA polymerases bind DNA tightly with K_d values varying from 5 to 70 nM (*9, 15, 37, 38, 40, 42*). According to the Pol X·DNA dissociation constant determined in this study, as well as in previously published reports (*26, 28*), Pol X seems to be among the polymerases with the highest affinity for DNA substrates. This tight DNA binding apparently contradicts our finding that the Pol X·DNA binary complex is nonproductive. However, the conditions of DNA binding assays do no reflect adequately the in vivo situation where dNTP is necessarily present. Therefore, even though the K_d^{DNA} value is smaller than K_d^{dNTP}, the relatively low concentration of available gapped DNA substrate and the abundance of dNTP shift the equilibrium toward the formation of the Pol X·dNTP complex. It is interesting to note that Pol X binds not only its physiological substrate (gapped DNA) but also double-stranded DNA (*43*). Since double-stranded DNA is present at much higher concentrations than gapped DNA in vivo, a mechanism of double-stranded DNA discrimination is required. In recent studies on Pol X−DNA interaction, it was proposed that the enzyme has two distinct modes for DNA binding (*28*). On the basis of the results of fluorescence titration experiments, Jezewska et al. hypothesized that Pol X interacts with a gapped DNA substrate using the entire DNA-binding site that consists of structural elements of both the catalytic and C-terminal subdomains. In contrast, interaction with double-stranded DNA might involve only one of the DNA-binding subsites of Pol X. We can speculate that these two DNA binding modes require different enzyme conformations. Perhaps formation of the Pol X·dNTP complex prevents Pol X from binding DNA in the double-stranded DNA binding mode and assists in recognition and binding of the gapped DNA substrate.

Previous studies of the kinetic order of substrate binding for several DNA polymerases have revealed that they possess a common sequential ordered mechanism. This finding was very anticipated, taking into account the template-directed nature of nucleotide incorporation catalyzed by DNA polymerases. Additionally, as processive enzymes, DNA polymerases should remain bound to DNA substrate to carry out processive polymerization, which also implies an ordered mechanism with DNA as the leading substrate. This proposed mechanism likely remains true for "classical" DNA polymerases. However, a number of recently discovered DNA polymerases with novel properties (*20*) might not have to follow the same presumed rationales. For instance, processivity is not a universally required feature of all DNA polymerases since most repair DNA polymerases, such as lesion bypass or BER polymerases, have evolved to incorporate a single dNTP at the site of DNA damage. While processivity necessitates a "DNA-first" order of substrate binding, a purely distributive polymerase would possibly be capable of binding dNTP as the first substrate. Even though an ordered "dNTP-first" binding mechanism would not be logical for mildly processive polymerases, they may still deviate from the classical DNA-first ordered mechanism and could, theoretically, display random sequential substrate binding. In addition to the lack of significant processivity, the determinative role of the templating base in the selection of incoming nucleotide could also be greatly reduced for low-fidelity DNA polymerases. A remarkable example of the weakened influence of the template can be found in Rev1, a member of DNA polymerase family Y, which utilizes a unique mechanism of nucleotide selection. This enzyme preferentially binds and incorporates dCTP regardless of the templating base (*17, 44, 45*). The crystal structure of the Rev1 ternary complex revealed that incoming nucleotide selection is dictated by the interaction of dCTP with an Arg324 residue, rather than base pairing with a dG template (*46*). Pol η, a low-fidelity DNA polymerase from family Y, can serve as another example of the reduced role of the DNA template in dNTP binding. As found in a recent crystal structure of the ternary complex of Pol η with the correct nucleotide and DNA substrate containing a cisplatin-induced lesion (*47*), the enzyme is able to preorient the incoming nucleotide and two metal ions in the active conformation even if the templating nucleotide is positioned outside the active site. Again, it has been suggested that the correct positioning of the incoming dNTP in the active site is mainly realized via interaction with the protein residues (*47*).

Similar to the above-mentioned low-fidelity polymerases, Pol X could also employ protein-mediated dNTP selection. For example, preferential affinity toward purine nucleotides could result from specific interactions with the active site residues. The structure of Pol X in complex with its substrates, which is not available at present, could improve our understanding of this substrate preference and, perhaps, of the altered order of substrate binding.

One could ask how general this altered mechanism is among other DNA polymerases. It would be too hasty to reach a definite conclusion that the altered binding order is universal to *any* extent. However, having Pol X as a precedent, we can conclude with certainty that this mechanism is *possible* for other DNA polymerases as well. Lesion bypass and repair polymerases could be potential candidates. Nucleotide prebinding might assist in the recognition of specific sites of DNA damage and facilitate their accurate bypass and/or repair. Overall, the findings of the studies presented here provide new directions toward an understanding of how DNA polymerases might employ distinct mechanisms to aid in their biological functions.

ACKNOWLEDGMENT

We thank Dr. M. Su for purification of the H115W mutant.

SUPPORTING INFORMATION AVAILABLE

Examples of global analyses of a representative steady-state inhibition data set and additional kinetic data. This material is available free of charge via the Internet at http://pubs.acs.org.

REFERENCES

1. McClure, W. R., and Jovin, T. M. (1975) The steady state kinetic parameters and non-processivity of *Escherichia coli* deoxyribonucleic acid polymerase I. *J. Biol. Chem. 250*, 4073–4080.
2. Fisher, P. A., and Korn, D. (1981) Ordered sequential mechanism of substrate recognition and binding by KB cell DNA polymerase α. *Biochemistry 20*, 4560–4569.
3. Majumdar, C., Abbotts, J., Broder, S., and Wilson, S. H. (1988) Studies on the mechanism of human immunodeficiency virus reverse transcriptase. Steady-state kinetics, processivity, and polynucleotide inhibition. *J. Biol. Chem. 263*, 15657–15665.
4. Tanabe, K., Bohn, E. W., and Wilson, S. H. (1979) Steady-state kinetics of mouse DNA polymerase β. *Biochemistry 18*, 3401–3406.
5. Wang, T. S. F., and Korn, D. (1982) Specificity of the catalytic interaction of human DNA polymerase β with nucleic acid substrates. *Biochemistry 21*, 1597–1608.
6. Beese, L. S., Friedman, J. M., and Steitz, T. A. (1993) Crystal structures of the Klenow fragment of DNA polymerase I complexed with deoxynucleoside triphosphate and pyrophosphate. *Biochemistry 32*, 14095–14101.
7. Sawaya, M. R., Pelletier, H., Kumar, A., Wilson, S. H., and Kraut, J. (1994) Crystal structure of rat DNA polymerase β: Evidence for a common polymerase mechanism. *Science 264*, 1930–1935.
8. Bryant, F. R., Johnson, K. A., and Benkovic, S. J. (1983) Elementary steps in the DNA polymerase I reaction pathway. *Biochemistry 22*, 3537–3546.
9. Chaudhuri, M., Song, L., and Parris, D. S. (2003) The Herpes Simplex Virus Type 1 DNA Polymerase Processivity Factor Increases Fidelity without Altering Pre-steady-state Rate Constants for Polymerization or Excision. *J. Biol. Chem. 278*, 8996–9004.
10. Cramer, J., and Restle, T. (2005) Pre-steady-state Kinetic Characterization of the DinB Homologue DNA Polymerase of *Sulfolobus solfataricus*. *J. Biol. Chem. 280*, 40552–40558.
11. Einolf, H. J., and Guengerich, F. P. (2000) Kinetic Analysis of Nucleotide Incorporation by Mammalian DNA Polymerase δ. *J. Biol. Chem. 275*, 16316–16322.
12. Roettger, M. P., Fiala, K. A., Sompalli, S., Dong, Y., and Suo, Z. (2004) Pre-Steady-State Kinetic Studies of the Fidelity of Human DNA Polymerase μ. *Biochemistry 43*, 13827–13838.
13. Washington, M. T., Johnson, R. E., Prakash, L., and Prakash, S. (2003) The Mechanism of Nucleotide Incorporation by Human DNA Polymerase η Differs from That of the Yeast Enzyme. *Mol. Cell. Biol. 23*, 8316–8322.
14. Washington, M. T., Johnson, R. E., Prakash, L., and Prakash, S. (2004) Human DNA Polymerase ι Utilizes Different Nucleotide Incorporation Mechanisms Dependent upon the Template Base. *Mol. Cell. Biol. 24*, 936–943.
15. Washington, M. T., Prakash, L., and Prakash, S. (2001) Yeast DNA Polymerase η Utilizes an Induced-Fit Mechanism of Nucleotide Incorporation. *Cell 107*, 917–927.
16. Carlson, K. D., Johnson, R. E., Prakash, L., Prakash, S., and Washington, M. T. (2006) Human DNA polymerase κ forms nonproductive complexes with matched primer termini but not with mismatched primer termini. *Proc. Natl. Acad. Sci. U.S.A. 103*, 15776–15781.
17. Howell, C. A., Prakash, S., and Washington, M. T. (2007) Pre-Steady-State Kinetic Studies of Protein-Template-Directed Nucleotide Incorporation by the Yeast Rev1 Protein. *Biochemistry 46*, 13451–13459.
18. Kumar, S., Lamarche, B. J., and Tsai, M.-D. (2007) Use of Damaged DNA and dNTP Substrates by the Error-Prone DNA Polymerase X from African Swine Fever Virus. *Biochemistry 46*, 3814–3825.
19. Prakash, S., Johnson, R. E., and Prakash, L. (2005) Eukaryotic translesion synthesis DNA polymerases: Specificity of structure and function. *Annu. Rev. Biochem. 74*, 317–353.
20. Yang, W., and Woodgate, R. (2007) What a difference a decade makes: Insights into translesion DNA synthesis. *Proc. Natl. Acad. Sci. U.S.A. 104*, 15591–15598.
21. Showalter, A. K., and Tsai, M.-D. (2001) A DNA Polymerase with Specificity for Five Base Pairs. *J. Am. Chem. Soc. 123*, 1776–1777.
22. Oliveros, M., Yanez, R. J., Salas, M. L., Salas, J., Vinuela, E., and Blanco, L. (1997) Characterization of an African Swine Fever Virus 20-kDa DNA Polymerase Involved in DNA Repair. *J. Biol. Chem. 272*, 30899–30910.
23. Lamarche, B. J., Kumar, S., and Tsai, M. D. (2006) ASFV DNA Polymerase X Is Extremely Error-Prone under Diverse Assay Conditions and within Multiple DNA Sequence Contexts. *Biochemistry 45*, 14826–14833.
24. Lamarche, B. J., Showalter, A. K., and Tsai, M. D. (2005) An Error-Prone Viral DNA Ligase. *Biochemistry 44*, 8408–8417.
25. Aravind, L., and Koonin, E. V. (1999) DNA polymerase β-like nucleotidyltransferase superfamily: Identification of three new families, classification and evolutionary history. *Nucleic Acids Res. 27*, 1609–1618.
26. Showalter, A. K., Byeon, I.-J. L., Su, M.-I., and Tsai, M.-D. (2001) Solution structure of a viral DNA polymerase X and evidence for a mutagenic function. *Nat. Struct. Biol. 8*, 942–946.
27. Maciejewski, M. W., Shin, R., Pan, B., Marintchev, A., Denninger, A., Mullen, M. A., Chen, K., Gryk, M. R., and Mullen, G. P. (2001) Solution structure of a viral DNA repair polymerase. *Nat. Struct. Biol. 8*, 936–941.
28. Jezewska, M. J., Bujalowski, P. J., and Bujalowski, W. (2007) Interactions of the DNA Polymerase X from African Swine Fever Virus with Gapped DNA Substrates. Quantitative Analysis of Functional Structures of the Formed Complexes. *Biochemistry 46*, 12909–12924.
29. Balbo, P. B., Meinke, G., and Bohm, A. (2005) Kinetic Studies of Yeast PolyA Polymerase Indicate an Induced Fit Mechanism for Nucleotide Specificity. *Biochemistry 44*, 7777–7786.
30. Deibel, M. R., Jr., and Coleman, M. S. (1980) Biochemical properties of purified human terminal deoxynucleotidyltransferase. *J. Biol. Chem. 255*, 4206–4212.
31. Martin, G., Moeglich, A., Keller, W., and Doublie, S. (2004) Biochemical and Structural Insights into Substrate Binding and Catalytic Mechanism of Mammalian Poly(A) Polymerase. *J. Mol. Biol. 341*, 911–925.
32. Williams, K. R., and Schofield, P. (1977) Kinetic mechanism of tRNA nucleotidyltransferase from *Escherichia coli*. *J. Biol. Chem. 252*, 5589–5597.
33. Pelletier, H., Sawaya, M. R., Kumar, A., Wilson, S. H., and Kraut, J. (1994) Structures of ternary complexes of rat DNA polymerase β, a DNA template-primer, and ddCTP. *Science 264*, 1891–1903.
34. Sheaff, R. J., and Kuchta, R. D. (1993) Mechanism of calf thymus DNA primase: Slow initiation, rapid polymerization, and intelligent termination. *Biochemistry 32*, 3027–3037.
35. Dunlap, C. A., and Tsai, M.-D. (2002) Use of 2-Aminopurine and Tryptophan Fluorescence as Probes in Kinetic Analyses of DNA Polymerase β. *Biochemistry 41*, 11226–11235.
36. Bakhtina, M., Roettger, M. P., Kumar, S., and Tsai, M. D. (2007) A Unified Kinetic Mechanism Applicable to Multiple DNA Polymerases. *Biochemistry 46*, 5463–5472.
37. Kuchta, R. D., Benkovic, P., and Benkovic, S. J. (1988) Kinetic mechanism whereby DNA polymerase I (Klenow) replicates DNA with high fidelity. *Biochemistry 27*, 6716–6725.
38. Patel, S. S., Wong, I., and Johnson, K. A. (1991) Pre-steady-state kinetic analysis of processive DNA replication including complete characterization of an exonuclease-deficient mutant. *Biochemistry 30*, 511–525.
39. Bose-Basu, B., DeRose, E. F., Kirby, T. W., Mueller, G. A., Beard, W. A., Wilson, S. H., and London, R. E. (2004) Dynamic Characterization of a DNA Repair Enzyme: NMR Studies of [methyl-^{13}C]Methionine-Labeled DNA Polymerase β. *Biochemistry 43*, 8911–8922.
40. Capson, T. L., Peliska, J. A., Kaboord, B. F., Frey, M. W., Lively, C., Dahlberg, M., and Benkovic, S. J. (1992) Kinetic characterization of the polymerase and exonuclease activities of the gene 43 protein of bacteriophage T4. *Biochemistry 31*, 10984–10994.
41. Fiala, K. A., and Suo, Z. (2004) Mechanism of DNA Polymerization Catalyzed by *Sulfolobus solfataricus* P2 DNA Polymerase IV. *Biochemistry 43*, 2116–2125.

42. Werneburg, B. G., Ahn, J., Zhong, X., Hondal, R. J., Kraynov, V. S., and Tsai, M.-D. (1996) DNA Polymerase β: Pre-Steady-State Kinetic Analysis and Roles of Arginine-283 in Catalysis and Fidelity. *Biochemistry 35*, 7041–7050.
43. Jezewska, M. J., Bujalowski, P. J., and Bujalowski, W. (2007) Interactions of the DNA polymerase X of African swine fever virus with double-stranded DNA. Functional structure of the complex. *J. Mol. Biol. 373*, 75–95.
44. Nelson, J. R., Lawrence, C. W., and Hinkle, D. C. (1996) Deoxycytidyl transferase activity of yeast REV1 protein. *Nature 382*, 729–731.
45. Washington, M. T., Minko, I. G., Johnson, R. E., Haracska, L., Harris, T. M., Lloyd, R. S., Prakash, S., and Prakash, L. (2004) Efficient and Error-Free Replication past a Minor-Groove N2-Guanine Adduct by the Sequential Action of Yeast Rev1 and DNA Polymerase ζ. *Mol. Cell. Biol. 24*, 6900–6906.
46. Nair, D. T., Johnson, R. E., Prakash, L., Prakash, S., and Aggarwal, A. K. (2005) Rev1 Employs a Novel Mechanism of DNA Synthesis Using a Protein Template. *Science 309*, 2219–2222.
47. Alt, A., Lammens, K., Chiocchini, C., Lammens, A., Pieck, J. C., Kuch, D., Hopfner, K.-P., and Carell, T. (2007) Bypass of DNA lesions generated during anticancer treatment with cisplatin by DNA polymerase η. *Science 318*, 967–970.

BI800731M